POLITECNICO DI TORINO
Repository ISTITUZIONALE

Seismic monitoring and cable supervision on optical data networks: requirements, challenges, and results

Original
Seismic monitoring and cable supervision on optical data networks: requirements, challenges, and results / Clivati, C., Ambrosone, R., Calonico, D., Carpentieri, F., Centonze, R., Donadello, S., Govoni, A., Herrero, A., Hovsepyan, M., Levi, F., Margheriti, L., Nespola, A., Notarstefano, F., Straullu, S., Vassallo, M., Virgillito, E., Curri, V.. - In: JOURNAL OF OPTICAL COMMUNICATIONS AND NETWORKING. - ISSN 1943-0620. - 18:8(2026), pp. 127-136. [10.1364/jocn.590258]

Availability:
This version is available at: 11583/3013627 since: 2026-09-14T13:08:55Z

Publisher:
Optica Publishing Group

Published
DOI:10.1364/jocn.590258

Terms of use:

This article is made available under terms and conditions as specified in the corresponding bibliographic description in the repository

Publisher copyright

(Article begins on next page)

08 October 2026

JOURNAL OF
Optical Communications
and Networking

Seismic monitoring and cable supervision on optical data networks: requirements, challenges, and results

Cecilia Clivati,[1,*] Renato Ambrosone,[2] Davide Calonico,[1] Francesco Carpentieri,[3] Rossella Centonze,[2] Simone Donadello,[1] Aladino Govoni,[4] Andrè Herrero,[4] Marianna Hovsepyan,[3] Filippo Levi,[1] Lucia Margheriti,[4] Antonino Nespola,[5] Federico Notarstefano,[1,2] Stefano Straullu,[5] Maurizio Vassallo,[4] Emanuele Virgillito,[2] and Vittorio Curri[2]

[1]Istituto Nazionale di Ricerca Metrologica, Strada delle Cacce 91, 10135 Turin, Italy
[2]Department of Electronics and Telecommunications, Politecnico di Torino, Turin, Italy
[3]Open Fiber, Rome, Italy
[4]Istituto Nazionale di Geofisica e Vulcanologia, Rome, Italy
[5]Links Foundation, Turin, Italy
*c.clivati@inrim.it

Received 14 January 2026; revised 27 March 2026; accepted 27 April 2026; published 27 July 2026

Optical fiber sensing on deployed cables is gaining significant interest as a means to enhance network integrity and expand environmental monitoring capabilities. To fully achieve these goals, sensing signals must coexist with data transmission. While phase and state-of-polarization analysis are promising candidates for this integration, their practical exploitation presents several challenges. Because these methods measure the integrated deformation along the entire cable, sensitivity is often limited by high environmental noise floors. Furthermore, event interpretation and localization require more sophisticated analytics than conventional distributed fiber sensing. Incorporating fiber sensing into standard network architectures also necessitates a novel telemetry management system capable of handling heterogeneous datasets, high data rates, and stringent synchronization requirements. We present progress on these aspects, based on multi-year analysis of fiber-sensing data collected in field environments. Our results confirm that integrated sensing achieves the sensitivity required to detect mid- and low-magnitude seismic events within a range of tens of kilometers from the fiber, holding the potential to support seismic monitoring services in terrestrial areas. Additionally, we demonstrate the detection and localization of anomalous vibrations and anthropogenic events and the development of an autonomous anomaly-detection tool suitable for real-time alerting. Finally, we outline the requirements for an advanced network management system designed to accommodate sensing alongside conventional telemetry, supporting the transition from proof-of-concept experiments to robust, large-scale applications. © 2026 Optica Publishing Group under the terms of the Optica Open Access Publishing Agreement

https://doi.org/10.1364/JOCN.590258

1. INTRODUCTION

Today, our society relies heavily on optical fiber networks. They are the major backbone for global communications, data exchange, and global trade and are therefore highly critical. In light of this, their integrity, both at a hardware and service level, is becoming a priority for network operators and government institutions more than ever before [1]. In parallel, their unique pervasiveness and growth prospects for the next decade [2] are opening opportunities for an emerging field of application, i.e., remote optical sensing. Remote optical sensing relies on the analysis of how a light beam's fundamental properties, e.g., its optical phase and state of polarization (SOP), change as a consequence of fiber deformations. Since optical fibers are intrinsically coupled to their surroundings, they act as sensors for environmental perturbations, including thermal fluctuations, seismic vibrations, and sound waves [3]. The ability to detect and interpret those deformations serves many different purposes. On one hand, it enables the protection of the infrastructure, e.g., by spotting anomalous vibration levels in the cable surroundings [4–7] that can anticipate malicious or unintentional cable damage. On the other hand, it allows

repurposing deployed optical cables to detect hazards such as earthquakes [8–12] or volcano activity [13,14], oceanographic phenomena [15–17], landslides [18], and tsunamis [19,20]; this is particularly attractive since optical fibers extend to the most remote regions of our planet, including ocean floors [21], where the deployment of conventional sensing tools is complex, costly, and frequently prone to failures.

Among the various techniques that have been proposed to detect cable deformations, distributed fiber sensing (DFS), based on a time-resolved analysis of backscattered light, has demonstrated remarkable sensitivity and spatial resolution [22], effectively turning deployed cables into an array of quasi-punctual sensors. Reported applications span from Earth sciences [13–16,20] to the supervision of human activities and infrastructures [23]. However, its high technological complexity and cost make it unsuitable for large-scale adoption. Moreover, limitations exist on its use on active transport networks, which are, in general, unidirectional and multiplexed. Unidirectionality requires DFS systems to bypass amplifiers and equalizers, hence impeding their use on ultra-long-haul cables where the architecture cannot be changed, e.g., subsea fibers that do not implement the high-loss loopback (HLLB) technology [19]. A consequence of this is also on the sensing range, limited to the maximum unrepeated distance granting an adequate signal/noise ratio (SNR), currently in the range of 170 km [24]. The compatibility with data channels cannot be ensured on a general basis, even though recent literature shows it is possible for some types of DFS [25] and on specific network architectures [26]. As a result, DFS is usually implemented on dedicated fibers, which makes it difficult to scale within the existing infrastructure. While impressive demonstrations have shown it capable of highly demanding tasks such as recording offshore tsunami formation [19], the technology remains better suited for specialized, high-resolution-demanding case studies rather than continuous, large-scale network supervision. This is particularly true in the current telecommunications landscape, where exponential growth in connectivity demand is pushing legacy fiber networks toward their ultimate capacity limits [27,28], leaving little room for dedicated sensing bandwidth.

Recently, it was shown that the analysis of the phase and SOP of laser signals propagated forward down the fibers enables the detection of their deformations while causing no disruption to simultaneous data transmission. Phase and SOP analysis have been applied to the detection of seismic [9–12,12,29,30] and oceanographic [17,31,32] phenomena, real-time infrastructure supervision [4,5,7], and vehicle traffic monitoring [33]. In general, these techniques are not able to resolve the location of disturbances, as they only provide information about the overall deformation of the fiber integrated along its full length. Hereafter, we will refer to these approaches as *integrated fiber sensing* (IFS). However, they present other advantages, such as simpler instrumentation, that translates into high integration potential and lower costs, a lighter amount of data that facilitates storage and processing, longer reach [17,30] and full compatibility with the existing network architecture, unlocking access to an unprecedented number of cable routes and environments (see Table 1 for a comparison between DFS and IFS in terms of performances and infrastructural constraints). All these advantages make them promising candidates for seamless integration in conventional telecom networks for permanent, global-scale monitoring.

Table 1. Comparison between the Main Features of Distributed and Integrated Fiber Sensing (DFS and IFS, Respectively)

	DFS	IFS
Space resolution	<10 m	No[a]
Range	170 km [24][b]	Unlimited
Data size ($f_s = 100$ Hz)	>50 GB/day [34]	<0.5 GB/day
Multiplexed networks	Open [19,25,26]	Yes
Unidirectional networks	No	Yes

[a]Limited to inter-span length with high-loss loopbacks (HLLBs) [17], better for some applications, see Section 3.B.
[b]Unlimited with HLLB technology [19].

The concept of integrating fiber sensing into the network infrastructure can be expanded from the hardware to the architectural layer. With a customized architecture, it would be possible to include in the telemetry management system recordings of the fibers' mechanical deformations alongside conventional telemetry data from the network equipment. A larger set of information from multiple sources can, in turn, enable more complete and dynamical knowledge of the network and its surroundings, supporting the development of alerting systems, self-healing functionalities, and dedicated maintenance plans. Those inputs can be exploited to develop a network digital twin (DT) that is able to predict evolution scenarios or capture potential failures [35] or hazards [36] and elaborate adaptation strategies [37] and proactive restoration [38] in a timely manner.

However, this idea presents a number of challenges. First, because phase and SOP analysis of transmitted optical signals only measure the integrated deformation of the cable, they are more sensitive to background noise than commercial distributed sensing systems and require complex strategies to extract the location of disturbances [4,9,17]. The ultimate sensitivity achievable with these techniques is still uncertain; comparisons between these two approaches, as well as with DFS, are scarce [4,39,40], and open questions remain on the relation between distributed or integrated strain recordings produced by fiber sensing and ground motion as measured by conventional seismometers [41–43]. Moreover, the ability to discern, in the complex signal recorded at the cable output, the origin of all the events contributing to its deformation requires complex data analytics tools that must excel in speed, efficiency, and reliability at the same time. Finally, the collection, combination, and orchestration of heterogeneous datasets—whether they be telemetry data produced by network elements or strain recordings produced by fiber sensing techniques—requires the design of a flexible, yet comprehensive, architectural framework based on a hierarchical and device-agnostic structure suited for disaggregated networks. Critical aspects include the ability to handle higher data volumes and rates than legacy telemetry management systems, data synchronization, latency, and data-stream management.

Addressing these challenges is mandatory to go beyond proof-of-concept experiments toward demonstrating complex use cases.

This paper shows progress in achieving these critical objectives based on several years of field acquisitions in different scenarios. Our testbed is described in Section 2. We focus on two specific use cases, i.e., seismic monitoring and cable supervision (Sections 3.A and 3.B). For each of these two use cases, we will describe the context, requirements, and relevant results we obtained. Finally, in Section 4, we discuss how those applications, with their different peculiarities, can be incorporated into a common architectural framework, focusing on the relevant requirements for an advanced telemetry management system to support joint communication and sensing.

A peculiar aspect of our work is its strong focus on terrestrial networks that, while challenging our ability to record faint events due to the high level of anthropic noise background, offer a richer diversity of case studies and a higher density of complementary sensing instruments for cross-comparison, validation, and interpretation of recorded events.

2. EXPERIMENTAL SETUP

The results reported in this paper were obtained on a live telecommunication cable that belongs to the regional ring network of the Italian telecommunication company Open Fiber. The fiber is used for data transmission at 100 Gb/s with quadrature phase-shift keying (QPSK) modulation between two medium-sized towns in a highly seismic area in central Italy. The fiber is mostly housed in the ground along a regional road or in conduits within the road infrastructure and contains a few aerial portions, hundreds of meters long. With continued data collection spanning about four years, this testbed enabled us to assess the detection of many types of perturbations, ranging from low- and mid-magnitude earthquakes, anthropogenic events (e.g., roadworks and vehicle passage), or the effect of natural events on aerial cables.

In 2021, we set up phase analysis using an ultrastable laser interrogator; we upgraded the setup in 2022 by installing a second laser interrogator for probing the fiber in counter-propagating directions, to assess the possibility of locating disturbances [10,44]. In 2025, a pair of polarization beam splitter (PBS)-based SOP analyzers was installed to record the SOP of two counter-propagating intensity-modulated, direct-detected (IMDD) data signals generated by conventional C-band 10G transceivers (TRXs) [40,45]. Phase and SOP occupy a single wavelength channel each, while the rest of the bandwidth is used for data traffic. The present work focuses on phase-based sensing due to the better interpretation we currently have of its results and the longer dataset available. However, availability of both phase- and SOP-based sensing will enable us to compare the response of SOP and phase to various types of solicitations that differ in strength, spectral content, and type of induced stress to the fiber.

3. RESULTS

A. Seismic Monitoring

Today, the deployment of conventional sensing grids (e.g., seismometers) is heterogeneous and mostly concentrated in high-seismic risk areas [46]. The lower sensitivity to weak seismicity outside those areas impairs the lower bound of seismic catalog completeness, which is a fundamental parameter for probabilistic seismic hazard assessment. Denser coverage would also help better resolve earthquake depth, identify active faults and their subsurface geometry, and improve the hazard assessment during aftershock sequences and swarms. In urban areas, it may enable the quantification of site-related shake amplification [47]. The density of the current terrestrial telecommunication grid is attractive for improving those studies. Considering regional ring fiber architectures across the EU territory, for instance, in many cases, each point is within a range of a few tens of kilometers from the closest optical fiber [21]. Given such high coverage and the described open challenges in seismic monitoring, we see the ability to detect weak earthquakes within a range of a few tens of kilometers as more relevant than the detection of large events, for which the existing sensing networks are already adequate. To assess the suitability of IFS for weak seismicity monitoring, it is important to verify the detection rate of events as a function of distance, magnitude, and environmental conditions for a meaningful number of occurrences.

During the period of operation, we recorded the occurrence of several earthquakes, covering a broad range of magnitudes, distances from the cable, and incident directions. This enabled us to quantitatively characterize the detection sensitivity as a function of those parameters and extract quantitative information from fiber recordings. For this study, we selected time windows corresponding to all regional earthquakes reported by the National Institute of Geophysics and Volcanology (INGV) [46] over a period of about four years (2022–2025) and assigned a quantitative score to the detection of each event by IFS. This step was performed manually by expert personnel according to criteria such as the ability to identify the arrival of P- and S-waves, their consistency with predicted arrival times, their spectral content, and their evolution over time. Our previous work [10], based on about 1.5 years of acquisition, already showed the ability of integrated phase sensing to record earthquakes with a sensitivity that is inversely proportional to the event distance and directly proportional to the magnitude, similarly to what is observed with conventional seismometers. Based on an updated catalog covering about four years, Fig. 1 shows the detection efficiency for weak-, mid-, and large-magnitude event classes as a function of their distance to the closest point of the cable. We observe a detection rate in excess of 30% for weak events up to a distance of 50 km, which extends further for mid and large magnitudes. We also note that, even though the present analysis is run on a considerably long dataset and the testbed is located in a highly seismic area, the histogram population for mid and large events is still scarce. This highlights the need for continued and long-term acquisitions that go beyond sporadic experiments when the focus is on characterizing the sensitivity of integrated sensing techniques.

Figure 2 shows how the recorded events are located with respect to the fiber: a clear cluster of events is located in the Apennine area, one of the most highly seismic regions of central Italy. The map also shows the location of seismometers of the National Seismic Network IV operated by INGV [46].

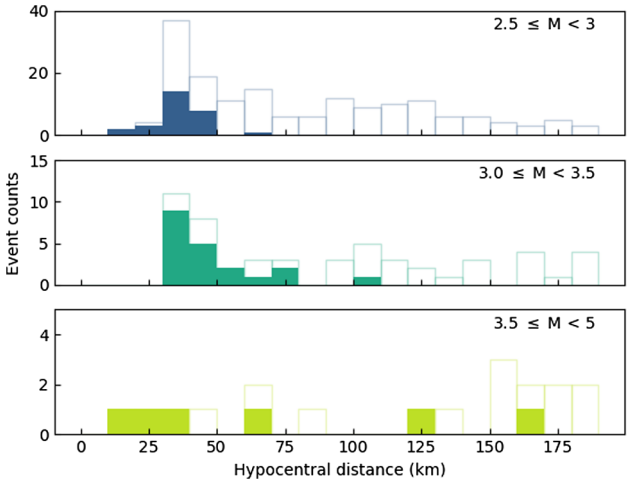

Fig. 1. Detection rate for events of low ($2.5 \leq M < 3.0$, top panel), mid ($3.0 \leq M < 3.5$, middle panel), and large ($3.5 \leq M < 5.0$, bottom panel) magnitude that occurred over the period of 2022–2025, as a function of their hypocentral distance to the closest point of the fiber. Filled (empty) bars indicate the counts of detected (total) events for each distance.

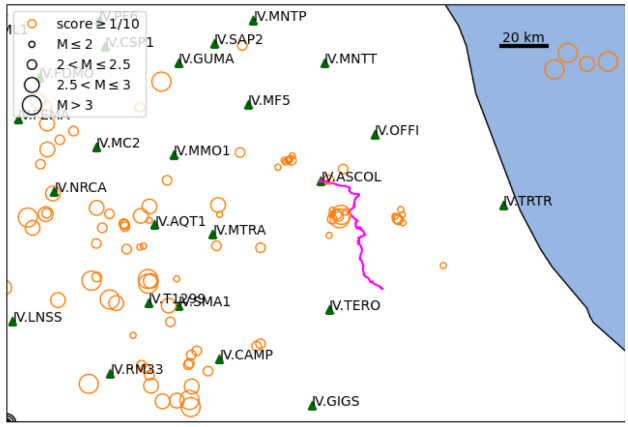

Fig. 2. Map of the cable layout (central Italy), with the location of the closest detected events (circles) and closest seismometers (triangles) of the INGV IV network [46].

In spite of the excellent coverage already provided by this network in the area, the optical fiber can still contribute due to its deployed nature and its ubiquitous presence.

The presence of a dense grid of nearby sensors also allows a reliable comparison between the waveforms recorded by the fiber and the actual ground motion. As an example, Fig. 3 shows the time trace of a magnitude 2.1 event at a distance of 19 km from the fiber recorded by phase-based sensing. The perturbation to the fiber is shown in terms of the time derivative of the accumulated phase (i.e., frequency fluctuations). The figure also shows the ground-motion recording of the seismometer IV.ASCOL of the Italian seismic network [46], located at one of the cable endpoints. A very good correspondence between the seismic-wave arrivals recorded by the two sensors can be observed, which opens the possibility of using fibers, in combination with conventional seismometers, to improve earthquake localization even in the lack of spatial resolution on the fiber. Functional analogy is also found between the ground velocity and the time derivative of phase variations. The scaling coefficient between quantities recorded by the two sensors is still a subject of debate and may be affected by different conditions, including the coupling between the fiber and the surrounding ground, or the incident direction [10,42,43]. In this respect, we note that large data collection catalogs, such

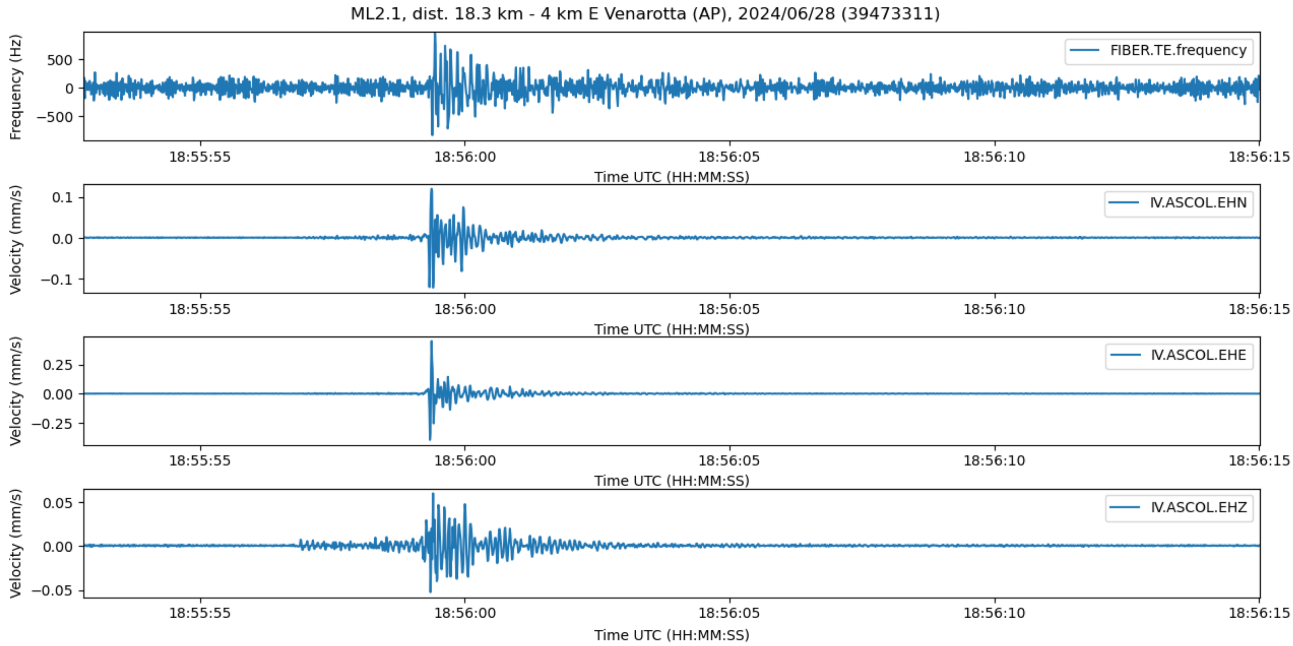

Fig. 3. Time trace of fiber and the three axes of the IV.ASCOL seismometer in the occurrence of a magnitude 2.1 event that happened 19 km north of the fiber on 28 June 2024. Fiber recordings are shown in terms of the time derivative of optical phase, i.e., in terms of a frequency shift. IV.ASCOL recordings are obtained from a three-axis velocimeter; channel codes EHN, EHE, and EHZ indicate the north–south, east–west, and vertical directions, respectively.

as the one we are building, are particularly relevant to this study, as they enable systematic comparisons and collective studies of detection ability as a function of incident direction and other geometrical parameters.

B. Cable Supervision

In addition to earthquakes, we observed signatures of other recurring events, among which we clearly identified: oscillations of suspended aerial portions of the cable triggered by wind gusts; maintenance and construction work; vehicle passage on specific points of the road mantle having high sensitivity, e.g., manholes or uneven asphalt coverage. Figure 4 shows the anomalous vibrations to which the aerial portion of the cable is subject during a storm. Comparison with wind and precipitation data for the area around the suspended fiber confirmed the occurrence of a perturbation with strong wind gusts during the same period. Anomalous oscillations of the cable persist for a few hours, are broadband, and their amplitude exceeds the normal background by one order of magnitude. A considerably different example is illustrated in Fig. 5. It shows (top panel) the phase-based recording of a perturbation produced by a vehicle passing close to a point where the road pavement is deteriorated, and the fiber is anomalously exposed. The perturbation lasts for 0.25 s and has an amplitude of 4 kHz, about five times smaller than the previous case.

Automated detection and classification of this kind of phenomenon are attractive in view of deploying remote infrastructural supervision. For instance, by monitoring the recurrence of vehicle detections over time, one can spot ongoing degradation of the road mantle; similarly, timely detection of anomalous vibrations in the cable proximity, e.g., during roadwork, can play a crucial role in avoiding damage to the cable and service disruption [6]. A prerequisite to any network supervision service based on the real-time detection of anomalies is the design of a suitable tool to spot and distinguish them from the persistent background vibrations considered normal behavior. Several works [5,48–50] have already addressed this issue, relying on both classical (e.g., short-term/long-term averaging) and machine learning algorithms, and considering both synthetic as well as real perturbation signatures. The use of synthetic signals provides a ground-truth reference against which

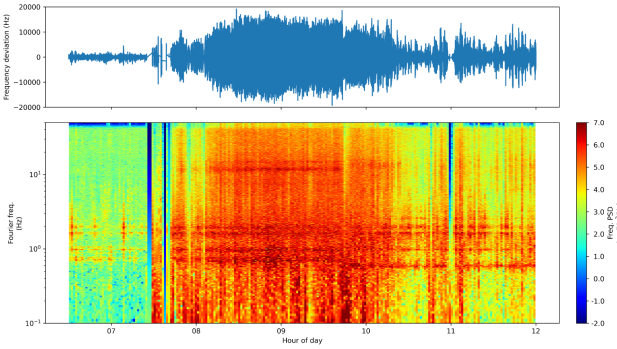

Fig. 4. Perturbation (time series and spectrogram) induced by a storm with strong wind gusts on the aerial fiber span. Deformations are plotted in terms of the time derivative of optical phase, i.e., frequency.

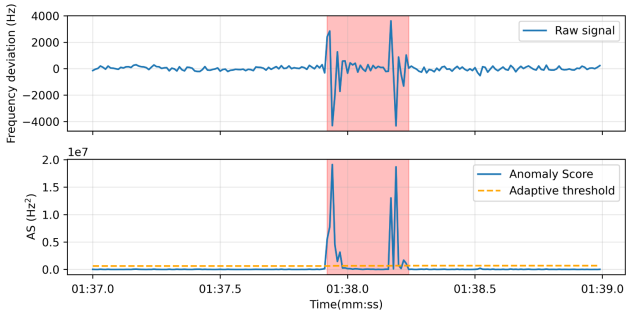

Fig. 5. Top panel: phase-based time series recorded during a vehicle passage on a degraded portion of the road mantle in the fiber proximity. Deformations are plotted in terms of the time derivative of optical phase, i.e., frequency. Bottom panel: anomaly score (AS) and adaptive threshold; the red-shaded region indicates the anomalous frame after merging anomalous samples occurring within a short time.

to assess the algorithm performance via metrics such as precision and recall and is useful in view of constructing a training dataset for supervised learning. On the other hand, a meaningful catalog of training events could be difficult to achieve and still may not capture the richness and diversity of real-world perturbation scenarios such as those shown in Figs. 3, 4, and 5. Validation against real signals on deployed fibers allows a more consistent assessment of the tool performances under dynamic and realistic signal/noise ratio conditions and offers the possibility of correlation with other metrics, such as quality of transmission (QoT) impairments. Among the possible strategies, we implemented an unsupervised learning pipeline based on a dense autoencoder architecture. Compared to classical methods, this approach grants the required flexibility to catch anomalies that differ substantially in terms of amplitude, duration, spectral content, and recurrence, as is the case of the examples shown. The workflow is designed to operate directly on continuous fiber sensing time series and does not require manual labeling of events, nor does it include parameters that are specific to the anomalies being searched for. To reduce computational effort, the algorithm can run on downsampled data. In our implementation, we adopt a sampling frequency of 100 Hz, which is a good compromise between the need to easily handle the whole dataset and the desire to capture fast transients such as the ones shown in Figs. 3 and 5. The processed signal is segmented using a sliding window with a length w and a unit step and then passed to the autoencoder. To train the autoencoder exclusively on background conditions, windows are ranked according to their root-mean-square variations, and only the 30% quietest windows are retained for training. This strategy enforces a data-driven definition of normal behavior and prevents contamination of the model by transient events. The autoencoder consists of a symmetric fully connected architecture with a low-dimensional bottleneck and is trained to minimize the squared reconstruction error on the selected quiet windows. Once trained, the model is applied in inference mode to the entire dataset. For each sample i, we calculate the error between the reconstructed signal $\hat{x}_i(t)$ and the original input signal $x_i(t)$ and then aggregate the contributions of all the k windows including that sample, yielding a continuous per-sample anomaly score computed as

$$\mathrm{AS}(t) = \frac{1}{k}\Sigma_{i=1}^{k}\left(x_i(t) - \hat{x}_i(t)\right)^2. \quad \textbf{(1)}$$

From the resulting AS time series, the rolling mean $\mu(t)$ and standard deviation $\sigma(t)$ are estimated over a 30 min window. Samples whose AS exceeds a fixed detection threshold,

$$\mathrm{AS}(t) > \mu + N\sigma(t), \quad \textbf{(2)}$$

are flagged as anomalous. In our tests, we used $N = 5$. Finally, a post-processing stage is applied to convert raw detections into physically meaningful events. Short-lived detections are pruned, and temporally adjacent anomalous segments are merged into single events, resulting in a compact and interpretable event catalog. Figure 5 shows how the algorithm performs in the representative case of the weak and short-duration anomaly produced by a vehicle passage. The lower panel shows the AS and the adaptive threshold, and the shaded region indicates the post-processed anomalous frame obtained after the pruning and merging steps. While not strictly necessary for the purpose of anomaly detection, the creation of these frames enables more complex analysis, finalized to investigate recurrent patterns and infer triggering phenomena [49]. In view of deploying a functional alert system, important aspects of concern are the threshold that defines anomalies versus normal behavior and the timeliness of the algorithm in detecting anomalies before they result in concrete damage. These aspects are controlled by algorithm parameters N and w, which can be set via a two-step process: one can first set the algorithm in a low-threshold (i.e., high-sensitivity) mode and analyze the correlation and mean time between recorded fiber anomalies and noticeable traffic disruption [5], such as flaps or bit error rate (BER) bursts. Then, N and w can be adapted to maximize precision and recall as best suited to the concrete application scenario and ensure that harmful events are predicted with proper advance, keeping in mind that the minimum system latency is w. It is important to note that, in all these cases, the algorithm would not be tuned with the ambition of detecting all anomalies, but only those resulting in appreciable impairments.

Another prerequisite for building an efficient infrastructural supervision system is the ability to pinpoint the location of disturbances. Unlike DFS, in IFS, this aspect requires some extent of signal processing, as raw SOP or phase signals only record the integrated deformation of the cable. Earlier work demonstrated per-span event localization exploiting high-loss loopback architectures in ultra-long-haul submarine networks [17,30], although this is not useful for cable supervision applications where at least kilometer-resolution is required. Localization uncertainty <10 km was demonstrated in the detection of fast transients induced by lightning strikes in aerial optical ground wire cables (OPWG) by measuring the time delay between perturbations experienced by SOP in the forward and return paths in a round-trip setup [51]. Building on our previous experiments conducted in controlled environments [9], we investigate the feasibility of exploiting correlations between counter-propagating beams recorded at opposite ends of a cable. This approach requires high-precision synchronization between the acquisition systems at the two cable endpoints. To achieve kilometer-scale localization accuracy, synchronization must be maintained at the 10 μs level, which exceeds the capabilities of standard network time protocol (NTP) implementations typically available at network nodes. To address this, we developed a custom hybrid software/hardware synchronization procedure that maintains alignment within 3 μs [44], thereby supporting sub-kilometer localization precision.

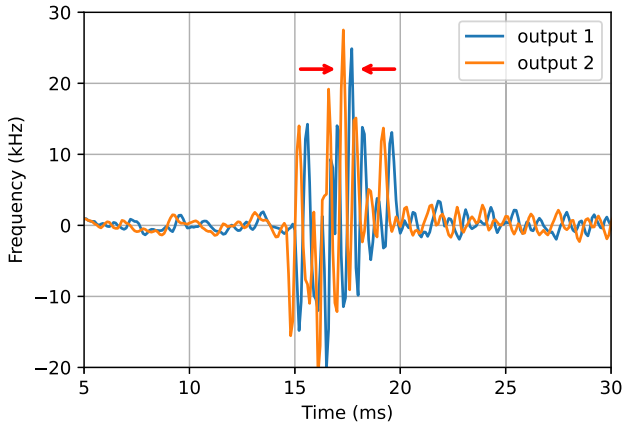

Fig. 6. Synchronous recordings of phase variations of a pair of counter-propagating laser beams collected at opposite cable endpoints. The delay between the two is consistent with the excitation position at the kilometer scale.

With synchronization established, the localization uncertainty is fundamentally limited by the event's spectral content [52]. This physical constraint hinders the localization of earthquake events whose spectral content rarely exceeds 40 Hz. Instead, the majority of events that are relevant to cable supervision (e.g., cable twisting or shaking, roadwork, construction, or vehicular traffic) can be localized due to their broader spectral signatures, which often extend into the kHz range. Figure 6 illustrates the synchronous phase-variation recordings of a tapping event measured at the two cable endpoints. The observed temporal delay between these signals is consistent with the physical location of the disturbance, demonstrating the concept of kilometer-scale localization by time-delay estimation.

Figure 7 shows localization results for a series of tapping events at an intermediate point of the cable where the fiber is accessible. The top panel shows phase variations recorded at opposite cable endpoints (blue and orange traces), while the bottom panel shows by color scale the cross-correlation function versus lag in adjacent 0.3-s-long sliding windows, with circles indicating the maximum for each window, i.e., the best time-delay estimate (TDE). Consistency of TDEs for tapping events is observed both between them and with the expected position of the excitation, with an uncertainty of 1 km (standard deviation) in a broad range of SNR conditions, including lower values than typical disturbances.

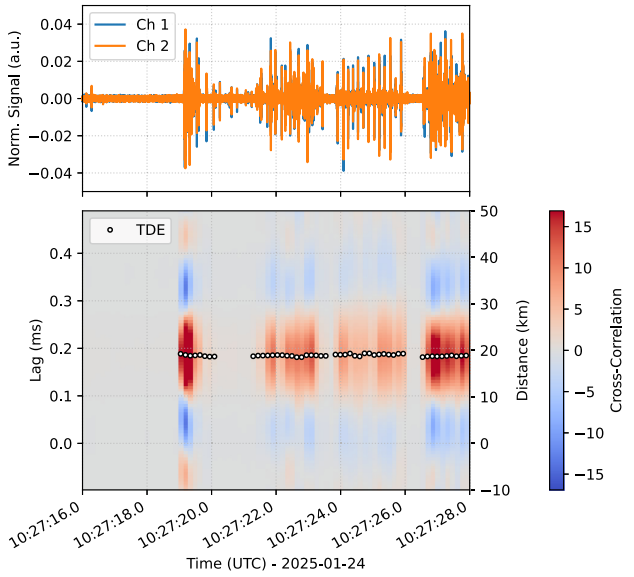

Fig. 7. Localization of tapping events at km 19 of the fiber. Top panel: time series (normalized signal) corresponding to recordings at opposite cable ends. Bottom panel: cross-correlation function versus lag in sliding windows with a duration of 0.3 s (right y-axis: lags rescaled to position along the fiber); circles indicate the maximum of cross-correlation for each window, corresponding to the event TDE.

4. BUILDING A VERSATILE, SENSOR-AGNOSTIC TELEMETRY MANAGEMENT SYSTEM

Applications of fiber sensing, such as those described in Section 3, can be fully enabled only if data are streamed, processed, and analyzed in flexible, yet structured architectures that support (i) scalability to multiple cables, multiple sensing nodes, and multiple users at a time; (ii) low-latency data interpretation also by combining different and potentially heterogeneous sources of information; and (iii) variable data formats, interrogation protocols, and streaming modalities as required by specific applications. With reference to the described use cases, seismic monitoring requires continuous fiber data streaming to institutional bodies that combine them with those from conventional sensing grids and run specialized analysis. Requirements are latency <1 s and sampling rates of up to 100 Hz. Instead, cable supervision applications take advantage of higher data rates to constrain the position of perturbations along cables; the same datasets, suitably downsampled to 100 Hz, can support anomaly detection as described in Section 3.B and correlation with data traffic impairments to identify disruption in a timely manner. A third relevant application scenario in network modeling is that fiber-sensing datasets can be used to include cable conditions in the computation of a network's DT. In general, its accuracy is inherently related to the amount of data upon which it is based. It is therefore important to use both sensing data derived from photonic techniques probing the cable (e.g., phase data from laser interferometry with alien laser interrogators, SOP data from dedicated acquisition boards, etc.) and telemetry data from conventional network elements (e.g., amplifier gain, temperature, optical signal/noise ratio, bit error rate, and SOP data from transceivers). An example is proposed in [53], where the

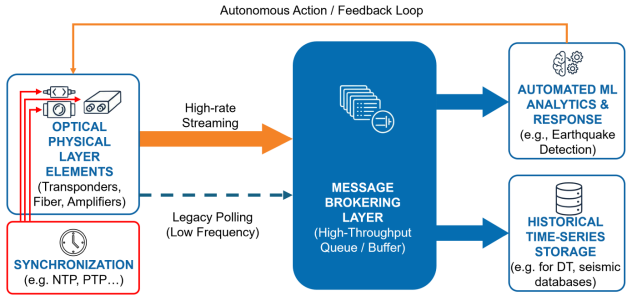

Fig. 8. Conceptual diagram of a high-frequency telemetry architecture for optical sensing.

accurate DT of an amplified line is built using typical telemetry data and a fully agnostic approach that does not include prior knowledge of network specifications. In [54], instead, the DT is constructed solely based on data obtained by probing an alien domain through a TRX exposing telemetry data, thereby enabling the use of the alien domain as a service.

To effectively implement these advanced monitoring scenarios, the underlying telemetry infrastructure must evolve beyond the assumptions of conventional network monitoring. Traditional telemetry systems are typically designed to collect low-rate performance indicators, often at timescales on the order of 1 s. By contrast, fiber-sensing applications generate time series at significantly higher rates (e.g., 100 Hz and above). In this context, telemetry is an enabling component of the sensing service itself. Our proposed architecture is shown in Fig. 8. This framework design considers the aspects discussed in previous sections and is based on strong interaction with potential users of the described technology for seismic monitoring and cable safety. It builds on the three pillars that are discussed in detail below.

A. Accurate Data Timestamping

Sensing data must be correlated by an accurate timestamp. Lack of synchronization impairs time-resolved analysis as required for event localization, and even more trivially, prevents any meaningful correlation and sensor fusion analysis. Today, NTP synchronization is supported by most servers and several, yet not all, network elements with uncertainty in the 10 ms range. Precise time protocols (PTPs), standardized as IEEE 1588 [55], would achieve sub-microsecond accuracy but require specific network configuration, which today restricts their use to specific applications [56]. Data timestamping at NTP-level accuracy is sufficient for DT development and network-modeling applications, while, as discussed in Section 3.B, event localization needs direct, hardware-based point-to-point synchronization of sensing nodes if a PTP is not available from the network provider. From this discussion, it follows that data must be timestamped by the devices that produce them. Timestamping at a centralized database is problematic, as the queuing process and data transmission through the network introduce uncontrolled and variable latencies and jitter, breaking causality relations in an unpredictable manner. Devices that do not support at least NTPs are not suitable for sensing applications unless supported by local timestamping agents.

B. Hierarchical Structure

Rather than forwarding all raw sensing samples directly to a single centralized platform, the system should include multiple telemetry instances deployed close to the devices, responsible for local acquisition, buffering, and first-stage organization of the data. These edge-level telemetry domains can then forward synchronized and structured data streams toward a higher-layer, aggregated telemetry plane, where cross-domain correlation, long-term storage, DT construction, and global analytics are performed. This hierarchical approach improves scalability, limits the impact of transport latency, and allows the telemetry system to remain device-agnostic while accommodating heterogeneous sensing sources. A layered architecture encompasses the possibility of organizing data into a local database before passing them to higher layers for offline processing and diagnostics, storage, or redistribution to broad user communities [57]. In general, data can be re-organized to support both event-based and/or continuous time series streaming to higher layers based on the different application(s), synchronization, and decimation requirements, also in view of long-term storage.

C. Message Brokering

A message-brokering layer must be introduced between data producers and downstream storage and analytics functions. A possible integration in optical networks, based on Apache Kafka, has been explored in [58]. The broker is essential not only to decouple producers from consumers but also to enable the transition from sample-wise telemetry to block-wise data handling, which is more suitable for high-rate sensing streams. Unlike common optical network performance counters, anomalies and events such as those presented in Figs. 5 and 6 evolve on sub-millisecond timescales, necessitating ingestion rates capable of sustaining thousands of samples per second without data loss. With the proposed approach, a sensing device first publishes data to the broker; then, the downstream pipeline can read and write them in blocks, rather than issuing one database transaction per sample. This significantly reduces overhead, improves transport and storage efficiency, and preserves the temporal structure of the signal. It also matches the operating model of existing ingestion tools, such as Telegraf [58], which can consume data streams from Kafka and write them efficiently into a database. In this sense, the broker acts as a shock absorber, smoothing the mismatch between data-generation and data-consumption rates while enabling scalable handling of high-rate sensing streams.

Including the above-mentioned aspects in modern telemetry management systems is a long process that requires the cooperation of different actors, real-world validation across diverse architectures and application scenarios, and a generalized evolution of the technology, e.g., replacement of obsolete equipment that does not support precise timestamping. Non-unique subsystem design choices are also possible. Therefore, we envision a comprehensive discussion on detailed implementation strategies involving all relevant players, including cable owners and operators, vendors, networking experts, and potential users from other communities, to transition from localized showcases to full-scale services.

5. CONCLUSION

We show how integrated fiber sensing in operational telecom cables can be leveraged for environmental monitoring and cable supervision purposes, addressing important prerequisites toward the development of a systematic network-sensing approach that goes beyond occasional and application-specific data recording. With exceptionally long datasets available, we were able to quantitatively assess the detection of weak seismicity in terrestrial fibers and develop automated recognition tools for anomaly detection in cable safety applications. We also discussed the feasibility of localizing the position of disturbances along the cable with km-level resolution. Importantly, the considered sensing approaches are fully compatible with simultaneous data transmission on multiplexed, unidirectional fiber backbones, thus being highly scalable and infrastructure agnostic. Finally, we discussed the critical aspects that future telemetry management systems must consider to enable the described use cases, focusing on aspects such as multi-user data fruition, scalability to multiple nodes, multiple techniques, disaggregated networks, and low-latency processing to address time-critical tasks.

This research contributes to the design of dual-purpose optical networks that simultaneously support communication and environmental monitoring, addressing the increasing demand for secure and adaptive infrastructures.

Funding. European Union project SENSEI (101189545).

Acknowledgment. Portions of this work were presented at ECOC 2025 in Copenhagen [59].

Disclosures. The authors declare no conflicts of interest.

Data availability. Data underlying the results presented in this paper are available in Ref. [60].

REFERENCES

1. D. Brake, *Submarine Cables: Critical Infrastructure for Global Communications* (2019).
2. TeleGeography, "2026 State of the Network Report" [accessed 24 July 2026], https://www2.telegeography.com/download-state-of-the-network.
3. Z. Zhan, "Distributed acoustic sensing turns fiber-optic cables into sensitive seismic antennas," Seismol. Res. Lett. **91**, 1–15 (2020).
4. E. Ip, Y.-K. Huang, G. Wellbrock, *et al.*, "Vibration detection and localization using modified digital coherent telecom transponders," J. Lightwave Technol. **40**, 1472–1482 (2022).
5. C. J. Carver and X. Zhou, "Polarization sensing of network health and seismic activity over a live terrestrial fiber-optic cable," Commun. Eng. **3**, 91 (2024).
6. M. Mazur, D. Wallberg, L. Dallachiesa, *et al.*, "Real-time monitoring of cable break in a live network using a coherent transceiver prototype," in *Optical Fiber Communication Conference (OFC)* (Optica Publishing Group, 2024), paper Tu3J.6.
7. P. Boffi, M. Fasano, A. Madaschi, *et al.*, "Joint communication and sensing in access networks for anthropic activities monitoring and real-time safety surveillance," in *IEEE Photonics Society Summer Topicals Meeting Series (SUM)* (2025).
8. N. J. Lindsey, T. C. Dawe, and J. B. Ajo-Franklin, "Illuminating seafloor faults and ocean dynamics with dark fiber distributed acoustic sensing," Science **366**, 1103–1107 (2019).
9. G. Marra, C. Clivati, R. Luckett, *et al.*, "Ultrastable laser interferometry for earthquake detection with terrestrial and submarine cables," Science **361**, 486–490 (2018).
10. S. Donadello, C. Clivati, A. Govoni, *et al.*, "Seismic monitoring using the telecom fiber network," Commun. Earth Environ. **5**, 178 (2024).

11. Z. Zhan, M. Cantono, V. Kamalov, *et al.*, "Optical polarization-based seismic and water wave sensing on transoceanic cables," Science **371**, 931–936 (2021).
12. A. Bogris, T. Nikas, C. Simos, *et al.*, "Sensitive seismic sensors based on microwave frequency fiber interferometry in commercially deployed cables," Sci. Rep. **12**, 14000 (2022).
13. G. Currenti, M. Allegra, F. Cannavò, *et al.*, "Distributed dynamic strain sensing of very long period and long period events on telecom fiber-optic cables at Vulcano, Italy," Sci. Rep. **13**, 4641 (2023).
14. R. Maass, S. Schippkus, C. Hadziioannou, *et al.*, "Stacking of distributed dynamic strain reveals link between seismic velocity changes and the 2020 unrest in Reykjanes," J. Geophys. Res. Solid Earth **129**, e2023JB028320 (2024).
15. H. Matsumoto, E. Araki, T. Kimura, *et al.*, "Detection of hydroacoustic signals on a fiber-optic submarine cable," Sci. Rep. **11**, 2797 (2021).
16. D. M. Flores, E. D. Mercerat, J. P. Ampuero, *et al.*, "Identification of two vibration regimes of underwater fibre optic cables by distributed acoustic sensing," Geophys. J. Int. **234**, 1389–1400 (2023).
17. G. Marra, D. M. Fairweather, V. Kamalov, *et al.*, "Optical interferometry–based array of seafloor environmental sensors using a transoceanic submarine cable," Science **376**, 874–879 (2022).
18. J. Kang, F. Walter, P. Paitz, *et al.*, "Automatic monitoring of rock-slope failures using distributed acoustic sensing and semi-supervised learning," Geophys. Res. Lett. **51**, e2024GL110672 (2024).
19. M. Mazur, N. K. Fontaine, R. Ryf, *et al.*, "Submarine cable deep-ocean observation of mega-thrust earthquake and tsunami with 44,000 100-m spaced sensors," in *European Conference on Optical Communication (ECOC)* (2025).
20. H. Xiao, Z. J. Spica, J. Li, *et al.*, "Detection of earthquake infragravity and tsunami waves with underwater distributed acoustic sensing," Geophys. Res. Lett. **51**, e2023GL106767 (2024).
21. ITU, "Infrastructure connectivity map" [accessed 10 January 2026], https://bbmaps.itu.int/bbmaps/.
22. B. G. Gorshkov, A. E. Alekseev, M. A. Taranov, *et al.*, "Low noise distributed acoustic sensor for seismology applications," Appl. Opt. **61**, 8308–8316 (2022).
23. H. Wijaya, P. Rajeev, and E. Gad, "Distributed optical fibre sensor for infrastructure monitoring: field applications," Opt. Fiber Technol. **64**, 102577 (2021).
24. O. H. Waagaard, E. Rønnekleiv, A. Haukanes, *et al.*, "Real-time low noise distributed acoustic sensing in 171 km low loss fiber," OSA Continuum **4**, 688–701 (2021).
25. S. Guerrier, C. Dorize, K. Abdelli, *et al.*, "Distributed coherent sensing over deployed fibers for network as a sensor applications," J. Lightwave Technol. **43**, 1736–1745 (2025).
26. S. Pellegrini, L. Hernandéz-Martin, A. M. R. Brusin, *et al.*, "Experimental and simulative study on IM-DD transmission and large chirped-pulse DAS coexistence," J. Lightwave Technol. **44**, 1743–1753 (2026).
27. E. H. Caoui and A. Steck, "Content providers and the deployment of Internet infrastructure," Inf. Econ. Policy **71**, 101134 (2025).
28. P. J. Winzer, D. T. Neilson, and A. R. Chraplyvy, "Fiber-optic transmission and networking: the previous 20 and the next 20 years [Invited]," Opt. Express **26**, 24190–24239 (2018).
29. S. Noe, D. Husmann, N. Müller, *et al.*, "Long-range fiber-optic earthquake sensing by active phase noise cancellation," Sci. Rep. **13**, 13983 (2023).
30. L. Costa, S. Varughese, P. Mertz, *et al.*, "Localization of seismic waves with submarine fiber optics using polarization-only measurements," Commun. Eng. **2**, 86 (2023).
31. A. Mecozzi, M. Cantono, J. C. Castellanos, *et al.*, "Polarization sensing using submarine optical cables," Optica **8**, 788–795 (2021).
32. A. Mecozzi, C. Antonelli, L. Palmieri, *et al.*, "Observation of precursor of the Kamchatka earthquake by monitoring a fiber optical link in the Mediterranean Sea," in *European Conference on Optical Communication (ECOC)* (2025).
33. F. Usmani, A. D'Amico, S. Straullu, *et al.*, "A smart sensing grid for road traffic detection using terrestrial optical networks and attention-enhanced Bi-LSTM," J. Lightwave Technol. **43**, 4624–4634 (2025).
34. A. Wuestefeld, Z. J. Spica, K. Aderhold, *et al.*, "The Global DAS Month of February 2023," Seismol. Res. Lett. **95**, 1569–1577 (2023).
35. M. C. Mohamed, M. U. Masood, I. C. Dipto, *et al.*, "Network data based transfer learning failure prediction agent pre-trained using digital twin," in *International Conference on Optical Network Design and Modeling (ONDM)* (2025).
36. H. Awad, R. Bratovich, S. Straullu, *et al.*, "Experimental validation on using optical network-as-a-sensor for earthquake early warning," in *International Conference on Optical Network Design and Modeling (ONDM)* (2025).
37. V. Curri, "Digital-twin of physical-layer as enabler for open and disaggregated optical networks," in *International Conference on Optical Network Design and Modeling (ONDM)* (2023).
38. G. Malik, M. U. Masood, M. C. Mohamed, *et al.*, "Machine learning for predictive multi-event detection in fiber optic systems," in *IEEE International Conference on Machine Learning for Communication and Networking (ICMLCN)* (IEEE, 2025).
39. D. C. Bowden, A. Fichtner, T. Nikas, *et al.*, "Linking distributed and integrated fiber-optic sensing," Geophys. Res. Lett. **49**, e2022GL098727 (2022).
40. E. Virgillito, F. Notarstefano, R. Centonze, *et al.*, "In-field demonstration of multi-tech sensing on terrestrial optical data network using state of polarization and phase monitoring," in *European Conference on Optical Communication (ECOC)*, Copenhagen, Denmark, 2025.
41. S. Diaz-Meza, P. Jousset, G. Currenti, *et al.*, "Insights in nonlinear ground response in volcanic environments from distributed dynamic strain sensing," Sci. Rep. **15**, 32698 (2025).
42. S. Noe, K. B. Tuinstra, S. Klaasen, *et al.*, "Theoretical background for full-waveform inversion with distributed acoustic sensing and integrated strain sensing," Geophys. J. Int. **244**, ggaf406 (2025).
43. A. Fichtner, A. Bogris, T. Nikas, *et al.*, "Theory of phase transmission fibre-optic deformation sensing," Geophys. J. Int. **231**, 1031–1039 (2022).
44. S. Donadello, E. K. Bertacco, D. Calonico, *et al.*, "Embedded digital phase noise analyzer for optical frequency metrology," IEEE Trans. Instrum. Meas. **72**, 2005412 (2023).
45. E. Virgillito, S. Straullu, F. Aquilino, *et al.*, "Detection, localization and emulation of environmental activities using SOP monitoring of IMDD optical data channels," in *23rd International Conference on Transparent Optical Networks (ICTON)* (2023).
46. Istituto Nazionale di Geofisica e Vulcanologia (INGV), "Rete Sismica Nazionale (RSN)" (2005), http://terremoti.ingv.it/instruments/network/IV.
47. Z. J. Spica, M. Perton, E. R. Martin, *et al.*, "Urban seismic site characterization by fiber-optic seismology," J. Geophys. Res. Solid Earth **125**, e2019JB018656 (2020).
48. D. Rafique, T. Szyrkowiec, H. Grießer, *et al.*, "Cognitive assurance architecture for optical network fault management," J. Lightwave Technol. **36**, 1443–1450 (2018).
49. L. Sadighi, S. Karlsson, C. Natalino, *et al.*, "Deep learning for detection of harmful events in real-world, noisy optical fiber deployments," J. Lightwave Technol. **43**, 6092–6101 (2025).
50. S. Pellegrini, L. Minelli, L. Andrenacci, *et al.*, "Overview on the state of polarization sensing: application scenarios and anomaly detection algorithms," J. Opt. Commun. Netw. **17**, A196–A209 (2025).
51. D. Charlton, S. Clarke, D. Doucet, *et al.*, "Field measurements of SOP transients in OPGW, with time and location correlation to lightning strikes," Opt. Express **25**, 9689–9696 (2017).
52. H. Cramer, *Mathematical Methods of Statistics* (Princeton University Press, 1999).
53. G. Borraccini, A. D'Amico, S. Straullu, *et al.*, "Cognitive and autonomous QoT-driven optical line controller," J. Opt. Commun. Netw. **13**, E23–E31 (2021).
54. R. Ambrosone, A. D'Amico, R. Schips, *et al.*, "QoT digital twin for bridging physical layer knowledge gaps in multi-domain networks," in *Optical Fiber Communication Conference (OFC)* (Optica Publishing Group, 2025), paper W4G.3.

55. IEEE, "IEEE standard for a precision clock synchronization protocol for networked measurement and control systems," IEEE Std 1588-2019 (Revision of IEEE Std 1588-2008) (2020).
56. SAFRAN, "The significance of accurate timekeeping and synchronization in trading systems," White paper [accessed 15 December 2025], https://safran-navigation-timing.com/timekeeping-and-synchronization-in-trading-systems.
57. R. Belso, H. Mihai, M. A. Pedersen, *et al.*, "Fibre optic sensing security architecture—a SUBMERSE white paper (1.0)," Zenodo (2025) [accessed 11 March 2026], https://doi.org/10.5281/zenodo.14998707.
58. A. Sgambelluri, A. Pacini, F. Paolucci, *et al.*, "Reliable and scalable Kafka-based framework for optical network telemetry," J. Opt. Commun. Netw. **13**, E42–E52 (2021).
59. C. Clivati, S. Donadello, F. Levi, *et al.*, "Proactive sensing of environmental events through optical data networks: a path to intelligent resilience," in *European Conference on Optical Communication (ECOC)* (2025), paper W.03.06.4.
60. C. Clivati, "Dataset related to publication 'Seismic monitoring and cable supervision on optical data networks: requirements, challenges, and results'," Zenodo (2026) [accessed 25 July 2026], https://doi.org/10.5281/zenodo.21571950.